

## Efficient removal of phosphate from aqueous solution by burnt brick clay: static conditions

T.P.K. Kulasooriya<sup>a,b</sup>, Namal Priyantha<sup>a,b</sup>, A.N. Navaratne<sup>a,b</sup>, Anushka Bandaranayake<sup>b</sup>, Linda B.L. Lim<sup>c,\*</sup>

<sup>a</sup>Department of Chemistry, Faculty of Science, University of Peradeniya, Peradeniya, Sri Lanka, Tel. +9471 6826502; email: kulasooriyat@yahoo.com (T.P.K. Kulasooriya), Tel. +9471 8672632; email: namal.priyantha@yahoo.com (N. Priyantha), Tel. +9481 2394430; email: ayanthi.pdn@gmail.com (A.N. Navaratne)

<sup>b</sup>Postgraduate Institute of Science, University of Peradeniya, Peradeniya, Sri Lanka, email: anushkabandaranayaka@gmail.com

<sup>c</sup>Chemical Sciences Program, Faculty of Science, Universiti Brunei Darussalam, Jalan Tungku Link, Gadong, Brunei Darussalam, email: linda.lim@ubd.edu.bn

Received 13 June 2020; Accepted 3 March 2021

### ABSTRACT

Phosphate species, the main nutrient pollutant, contributes to eutrophication, causing harmful effects to aquatic life. Adsorption of phosphate from synthetic solutions prepared using  $\text{KH}_2\text{PO}_4$  shows 87% removal from  $10.0 \text{ mg L}^{-1}$  phosphate solution at 1:10 adsorbent/solution ratio, under the optimized conditions, by brick clay particles burnt at  $200^\circ\text{C}$  (BBC). Based on error analysis and regression coefficients, removal of phosphate by BBC could be explained by the Freundlich isotherm model in general and the Dubinin–Radushkevich (D–R) isotherm at high concentrations. More importantly, the saturation capacity ( $q_{\text{max}}$ ) determined by the D–R model is  $4,531 \text{ mg kg}^{-1}$ , which is significantly higher when compared to other adsorbents reported. Further, kinetics data show the validity of the pseudo-second-order model, with the rate constant ( $k'$ ) and initial adsorption rate ( $h_0$ ) of  $2.25 \times 10^{-2} \text{ kg mg}^{-1} \text{ min}^{-1}$  and  $156 \text{ mg kg}^{-1} \text{ min}^{-1}$ , respectively. The use of BBC accelerates the mass transfer process providing more vacant sites for adsorption of phosphate, while unbound Ca and Fe particles may also result in strong bonds with phosphate species.

**Keywords:** Adsorption; Burnt brick clay; Phosphate; Static models; Characterization

### 1. Introduction

Nutrient pollution of water resources contributed by activities of living beings, such as domestic sewage, is further intensified by the use of phosphate minerals in agricultural and industrial activities. A slight increase in nutrient concentration entering the water body would increase the rate of eutrophication, which would occur when the concentration of phosphorous in a water body becomes higher than  $0.02 \text{ mg L}^{-1}$  [1]. Phosphorous is an element of concern because even small amounts of

phosphate would result in the growth of biological organisms, promoting harmful effects to the ecosystem.

Algal growth in water that would enhance with an increase in the dissolved phosphate levels [2] can be overcome by the removal of phosphate from contaminated wastewater before it reaches reservoirs. This can be achieved by physicochemical, biological and adsorption processes [3]. Chemical precipitation with alum, lime and iron salts, often used for the removal of phosphate from wastewater, are less effective at low concentration levels of phosphate [4,5]. On the other hand, biological methods are effective to remove only 10%–30% of phosphate [3], and

\* Corresponding author.

hence such methods would not reduce phosphate levels to the discharge limits. According to the Gazette of Sri Lanka, the tolerance limit of dissolved phosphate (as P) for the discharge of industrial waste into inland surface waters is  $0.5 \text{ mg L}^{-1}$ . Adsorption techniques have thus become attractive for phosphate removal as they are superior to existing chemical or biological methods in many respects, such as environmentally friendliness, low-cost, high uptake capacity, faster regeneration kinetics and greater selectivity [2]. Recent reports in this direction include the use of adsorbents, such as mine waste, fly ash, skin split waste, coir pith, sugarcane bagasse and sawdust, in their natural or modified forms [3–8]. Although much research has been done on metal ion removal by raw and modified brick clay, the focus on phosphate removal by modified brick clay has not been paid much attention [9,10]. Nevertheless, individual clay minerals have been researched upon for their phosphate removal ability [11,12]. The use of brick particles incorporated with waste and minerals for the removal of phosphorus and nitrogen indicates that brick clay has the potential for *in-situ* remediation of the aquatic environment [13]. Most importantly, the characterization of phosphate adsorbed brick clay has shown higher strength than normal fired brick. The highest strength has been reported at the equilibrium pH of 7 for brick clay fired at  $500^\circ\text{C}$  [10].

The present study is mainly based on the use of three adsorbents, brick clay, feldspar and dolomite, to investigate their phosphate removal ability. Feldspar and dolomite were selected by considering their natural availability in large quantities in different locations in Sri Lanka and the possibility of having affinity toward phosphate in the aqueous medium through complex formation due to their mineral composition with positively charged species. Further, both dolomite and feldspar are stages of aging soils that can be used to compare the removal ability of brick clay. The main part of the study focused on the use of heat-treated brick clay particles for the removal of phosphate, investigation of adsorption characteristics of phosphate, which include the determination of optimum conditions for the interaction under static conditions, and study of the kinetics of adsorption and desorption. Adsorption equilibrium studies were then extended to investigate the validity of different isotherm models in order to get an insight into the adsorption behavior of the system.

## 2. Materials and methods

### 2.1. Materials

Standard phosphate solutions were prepared using analytical grade  $\text{KH}_2\text{PO}_4$ . In each measurement, commercially available charcoal was used to remove colored substances, and the effect of charcoal was corrected against a blank run. The concentration of the phosphate level in all solutions was measured using the Vanadomolybdo-phosphate method at 420 nm. All experiments were conducted in triplicate, and the average results were reported. Brick clay, feldspar, and dolomite were obtained from the Central Province, Sri Lanka. The main adsorbent used in this study, unfired brick clay, was collected from a kiln located at Gelioya, Sri Lanka, on which many characterization experiments have carried out previously [14,15].

The surface of unfired brick clay was modified at the laboratory by applying known constant heat for the surface to have identical conditions throughout the experiment. All three adsorbents were crushed using a ball mill and pieces of diameter ( $d$ )  $< 1.0 \text{ mm}$  were used for all experiments.

### 2.2. Instrumentation

Representative samples of brick clay were fired using Carbolite CTF 12/100/900 tube furnace, while a UV-vis spectrophotometer (Shimadzu-1800UV, Japan) was used to record the absorbance of solutions at the wavelength recommended in the Vanadomolybdate method, 420 nm at neutral pH. Metals present in adsorbents were determined using X-ray fluorescence (XRF) spectrophotometer (Fisherscope Model-DF500FG-456), while scanning electron microscopic (SEM) images were obtained using Oxford Instruments – EVO LS 15 (Zeiss, Germany) instrument.

### 2.3. Research design

#### 2.3.1. Parameter optimization

In order to select the best adsorbent for the experiment, the removal efficiency of phosphate from synthetic effluent solutions was determined with dolomite, feldspar and brick clay without any heat treatment. For this purpose, 50 mL of  $10.0 \text{ mg L}^{-1} \text{ PO}_4^{3-}$  solution was shaken at 150 rpm with each adsorbent separately for 10 min, and solutions were allowed to stand for 1.0 h to reach equilibrium. A mass of 0.10 g of charcoal was added to each sample, shaken, and filtered using  $0.45 \mu\text{m}$  filter paper to remove any color of the solution. Upon the color development for standards and samples, the absorbance of each sample was recorded at 420 nm, and the percentage removal was determined, where  $C_i$  is the initial concentration and  $C_f$  is the final concentration:

$$\text{Percentage removal} = \frac{C_i - C_f}{C_i} \times 100\% \quad (1)$$

The effect of the firing temperature of brick clay particles was studied by varying the firing temperature from unfired to  $200^\circ\text{C}$ , to check the effect of adsorbent after the evaporation of water and different organic constituents present in the material, which may alter the binding capabilities of the adsorbent. The burning process was carried out for 4.0 h to confirm having equally burned adsorbent for subsequent experiments. Similarly, the effect of contact time was determined for fired brick clay samples, and the most efficient adsorbent was selected. Further, for optimization of shaking and settling times, 50 mL of  $10.0 \text{ mg L}^{-1} \text{ PO}_4^{3-}$  solution was shaken with 5.00 g of brick clay particles burnt at the optimum firing temperature of  $200^\circ\text{C}$  (BBC) by varying respective contact time from 0 to 90 min, while keeping other parameters constant.

#### 2.3.2. Adsorption isotherms

Phosphate solutions of a series of concentrations ( $2\text{--}1,000 \text{ mg L}^{-1}$ ) were treated with BBC in 1:10 solid/

solution ratio, and the optimum shaking and settling time periods were allowed for each system to reach equilibrium. Solutions were filtered, color development reagents were added, and the remaining concentrations were determined. The data were fitted to linearized forms of different adsorption isotherm models [16].

### 2.3.3. Kinetics modeling

To investigate the validity of kinetics models, experiments were conducted for BBC by withdrawing 35.0 mL volumes of samples from 20 different sample containers prepared under identical conditions by shaking 50 mL of 10 mg L<sup>-1</sup> phosphate solution with 5.0 g of BBC. Samples were withdrawn at every 1.0 min interval for 20 min before the system reached equilibrium. They were immediately filtered, and the remaining concentration of phosphate was determined.

### 2.4. Desorption of phosphate from the adsorbent

After completion of adsorption experiments, phosphate-adsorbed BBC samples were allowed to air-dry until a constant mass was obtained. Thereafter, 1.00 g of phosphate-adsorbed BBC was shaken with 50.0 mL of pH-adjusted water for 1.0 h, and allowed to stand for another 1.0 h. The concentration of phosphate leached out was determined to calculate the extent of desorption. The experiment was repeated for different initial pH values

in the range of 2–12, adjusted with HNO<sub>3</sub> (0.1 mol dm<sup>-3</sup>) and NaOH (0.1 mol dm<sup>-3</sup>).

## 3. Results and discussion

### 3.1. Bulk characterization of adsorbents

According to the XRF patterns, in addition to the main elements, Fe and Si, present in brick clay, trace elements, such as Mn and Ti, are present while dolomite contains mainly Ca and Fe (Ca is predominant). On the other hand, feldspar contains many metal ions, including Si, K, Ca, Fe Br, Rb, Sr, and Ag (Fig. 1). According to the XRD studies, it is determined that brick clay used for this investigation consists of aluminosilicates in addition to normal constituents, such as quartz and topaz, although XRF is not able to identify the presence of Al [17].

### 3.2. Selection of an adsorbent and parameter optimization

Based on the extent of removal of phosphate from synthetic solutions prepared in the laboratory by three natural adsorbents, unfired brick clay was found to be the most efficient adsorbent with more than 80% removal under experimental conditions employed (Fig. 2). Feldspar and dolomite are considered to have ion-exchange properties, resulting in reactions that would take place on the surface which make them used as adsorbents for

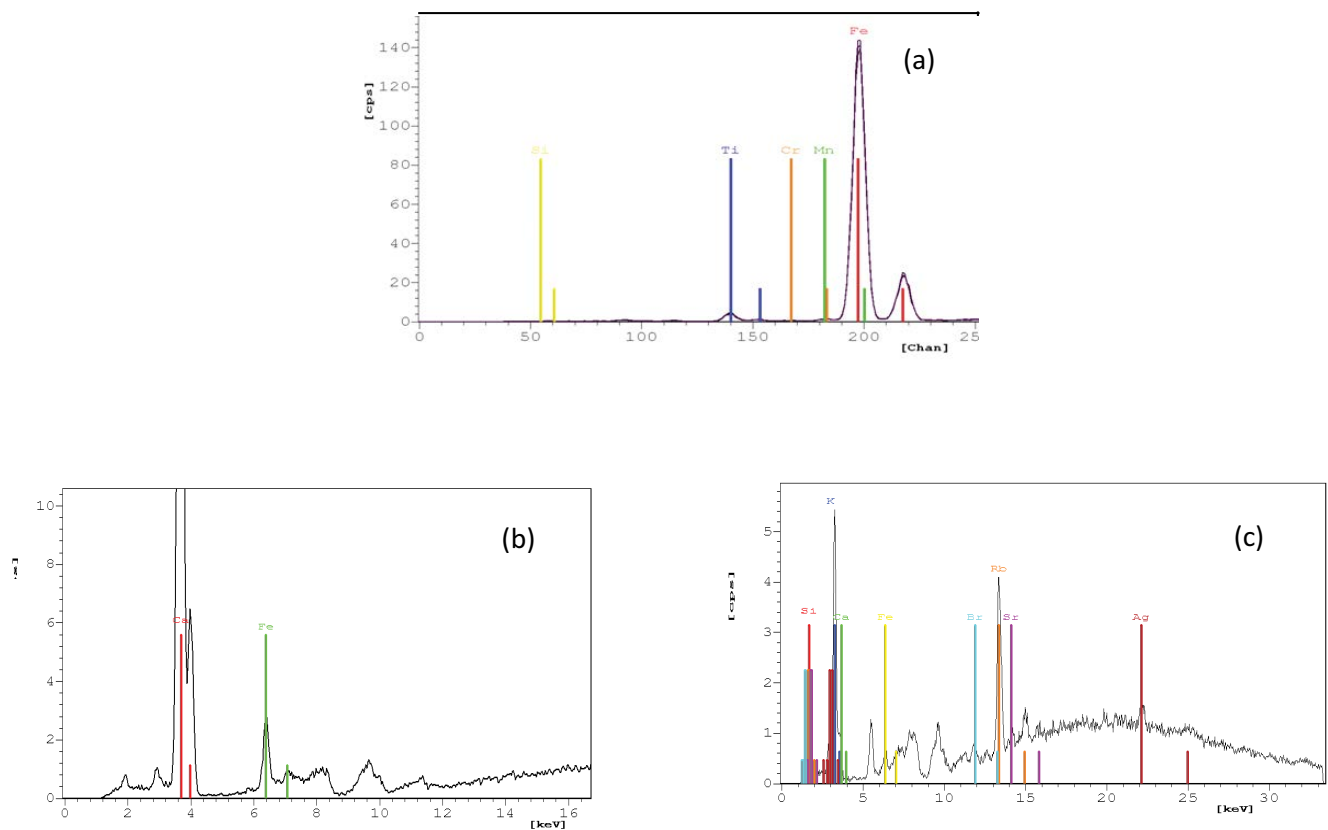


Fig. 1. XRF spectra of adsorbent samples: (a) brick clay, (b) dolomite, and (c) Feldspar. Lines indicate specific peak locations of respective elements.

pollutant removal [18,19]. Further results reveal that the ability of BBC for the removal of phosphate from the aqueous medium is superior to unfired brick clay. However, ion exchange would not probably be the main mode of mass transfer for the adsorption of phosphate.

Although not detected through XRF, Al, Ca and Mg are prominent metal ions present in the soil. Therefore, the removal of  $\text{PO}_4^{3-}$  by adsorbents would probably be due to

adsorption and/or a reaction with BBC particles resulting in chemical bond formation with such metals. Considering the high extent of removal of phosphate by BBC, parameters, namely firing temperature of adsorbent, shaking time, and settling time, were optimized for its removal by BBC.

Since the study focused on  $\text{H}_2\text{PO}_4^-$  and  $\text{HPO}_4^{2-}$  ions, the initial solution pH was remained neutral throughout the study. Further, throughout the optimization process, adsorbent dosage was taken as 5 g per 50 mL of solution, by considering its percentage removal of 80%, which is much acceptable for the optimization stage.

According to Fig. 3a, it is clear that the percentage removal is not significantly affected by the temperature of the treatment. Further, optimization of contact time results in 30 min shaking and a very short settling time (Figs. 3b and c).

Treatment of brick clay, pre-fired at different temperatures, with deionized water at ambient temperature leaches out soluble or loosely bound Al from the brick matrix. The leaching ability of Al decreases with the firing temperature of brick clay as shown in Fig. 4, which indicates that the concentration of Al in the aqueous suspension of either unfired brick clay or clay fired at  $100^\circ\text{C}$  is about  $6.0 \text{ mg L}^{-1}$ , which is equivalent to the leaching of 6.0 mg of Al by 1.0 kg of clay. The extent of Al leached out is drastically decreased down to very low levels for brick clay fired at temperatures above  $200^\circ\text{C}$ . Transformation of the layered structure of clay, which is responsible for the plasticity effect of raw clay where certain Al ions are loosely bound, to form a rigid three-dimensional network upon

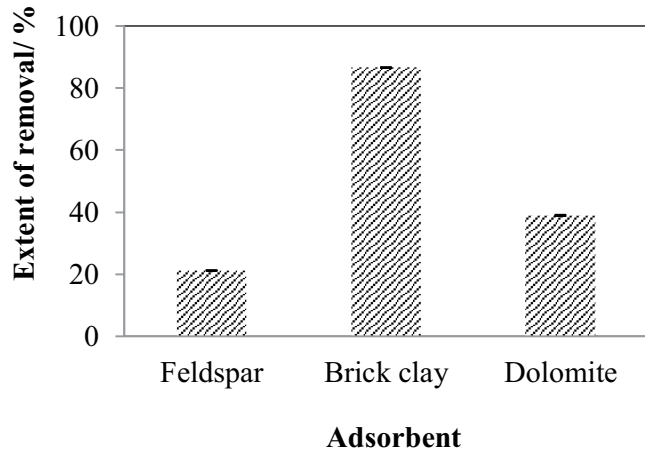


Fig. 2. Extent of removal of phosphate using various adsorbents (50.0 mL of  $10.0 \text{ mg L}^{-1} \text{ PO}_4^{3-}$  solution, 5.00 g of each adsorbent). Error bars at the top of the bar indicate standard deviation.

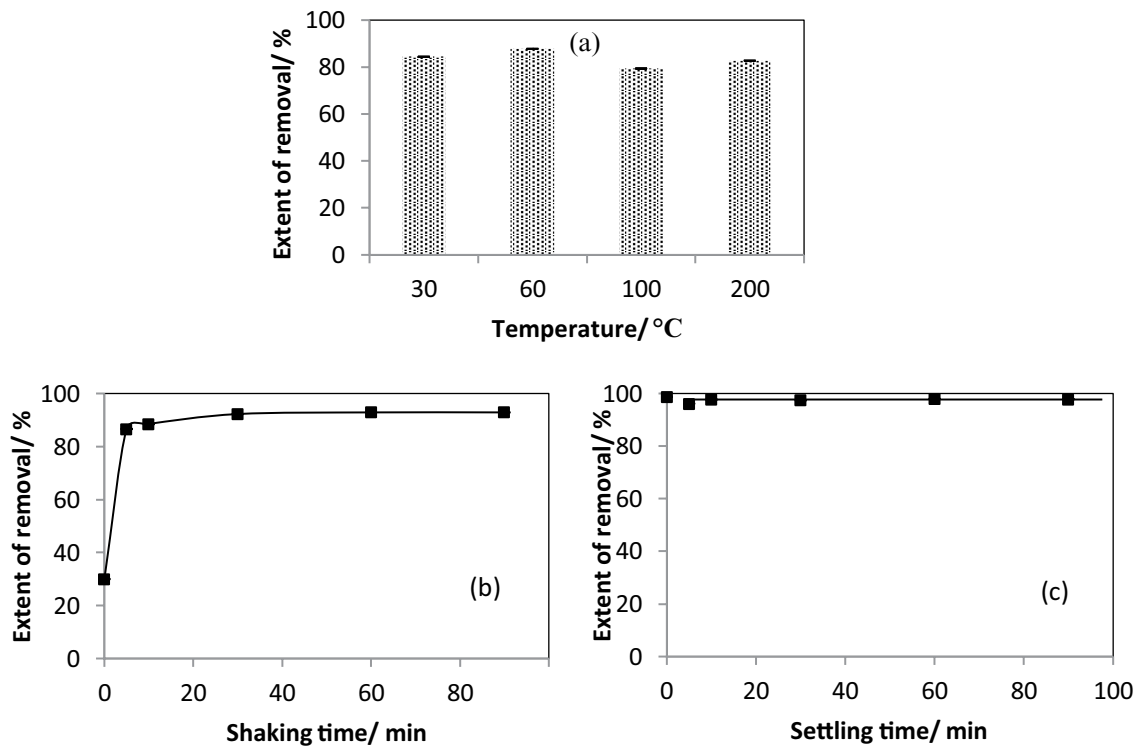


Fig. 3. Extent of removal of phosphate (a) brick clay fired at different temperatures, (b) optimization of shaking time with 1.0 h settling time, and (c) settling time at optimized shaking time (50.0 mL of  $10.0 \text{ mg L}^{-1} \text{ PO}_4^{3-}$  solution, 5.00 g of each adsorbent). Error bars at the top of the bar indicate standard deviation in panel (a), and error bars were not indicated in panels (b and c) due to insignificant uncertainty.

firing, would be a probable reason for much decreased leaching levels of Al. Thus, the interaction of kiln-fired brick used in construction activities, which is fired at temperatures greater than 400°C, with water would not leach significant levels of Al. Consequently, this interaction would not probably pose any risk to human health under normal atmospheric conditions. Consequently, brick clay fired at 200°C (BBC), the lowest firing temperature which gives the lowest extent of leaching of Al, was selected for phosphate removal experiments.

Surface functional groups of brick clay are attributed to a change in the chemistry with firing. Although the surface area remains constant up to 200°C, it drastically decreases with increasing firing temperature [17]. On the other hand, it has been reported that the release of Al and Fe decreases with an increase in firing temperature up to 200°C, while leaching of Ca is much higher. The high turbidity of solutions of unfired brick clay suspensions is due to the clay nature which is present even if it is fired at 100°C, limiting its applicability in real applications [14]. On the other hand, brick clay treated at 200°C or higher temperatures has been shown to have a strong ability for the removal of heavy metal ions and dyes, providing support for the

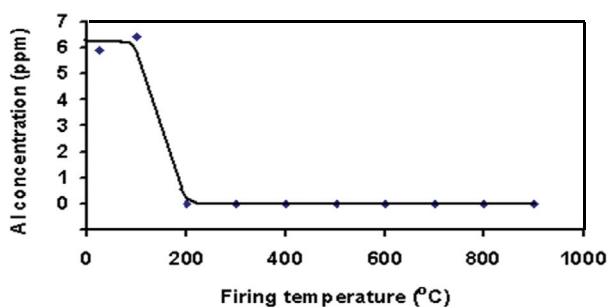


Fig. 4. Concentration of aluminum in the supernatant after interaction of brick clay fired at different temperatures with distilled water and (5.0 g brick clay, 50.0 mL distilled water, 10 min stirring, and 2.0 h settling).

selection of 200°C as the optimum firing temperature for phosphate removal [15,20–22]. SEM images recorded before and after adsorption of phosphate on BBC indicate an irregular adsorbent surface providing a large surface area for interaction with phosphate, leading to a significant change in the adsorbent surface after phosphate adsorption (Fig. 5).

### 3.3. Adsorption isotherms

The amount of phosphate adsorbed by brick clay fired at 200°C plotted against the initial concentration provides a clear indication of the validity of type II isotherm according to IUPAC classification (Fig. 6), describing the reversible physisorption on non-porous or macroporous adsorbents with strong and weak adsorbate–adsorbent interactions [23]. It is important to stress the fact that the BBC surface would not reach saturation even at concentrations as high as 1,000 mg L<sup>-1</sup>. The shape is a result of unrestricted monolayer–multilayer adsorption. More gradual curvature is an indication of a significant amount of overlap of monolayer and multilayer coverage, indicating that the adsorption of phosphate on BBC is not limited to monolayer coverage.

Using the equilibrium concentration of the same experimental data, the validity of different adsorption isotherm models was checked to identify the adsorption behavior (Table 1). Regression coefficients determined using the linearized relationships of four adsorption isotherms show that the removal of phosphate by brick clay could be explained by the Freundlich isotherm model and the Dubinin–Radushkevich (D–R) isotherm at higher concentrations, and Langmuir isotherm at lower concentrations. The Langmuir adsorption isotherm is mainly applied for low concentrations, defined for a chemisorption process leading to a monolayer. Assuming that adsorption can only occur at a finite number of definite localized sites with no lateral interaction [24].

With the application of adsorption isotherm models, different error functions were used to select the best model to describe the adsorption behavior (Table 2).

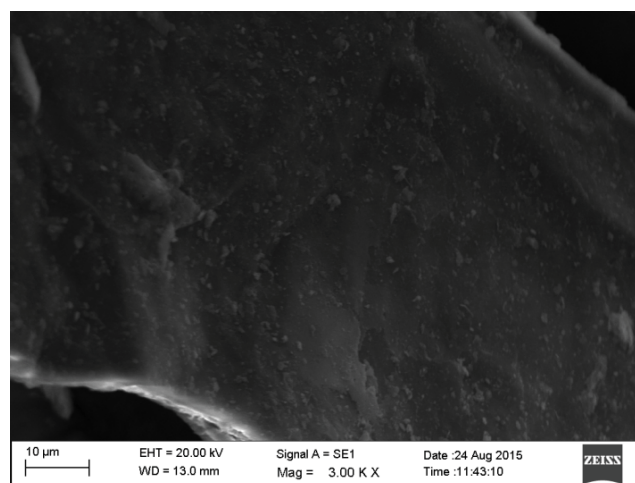
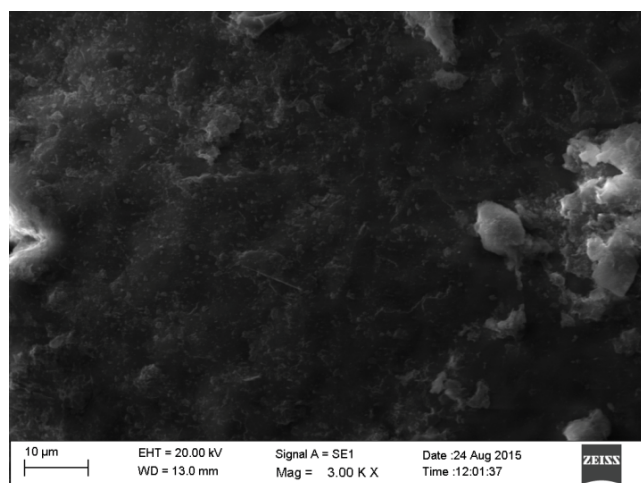


Fig. 5. SEM images for brick clay fired at 200°C before adsorption (left), and after adsorption of phosphate (right).

The results obtained are shown in Table 3 [26]. Higher error values of a model indicate that it is not suitable in explaining phosphate adsorption.

When considering the regression coefficient values (Table 1) and different error functions (Table 3), it is clear from smaller ARE values that the removal of phosphate by BBC could be explained by the Freundlich isotherm model in general and the D–R isotherm at high concentrations, and thus results were further analyzed to determine adsorption parameters.

According to the adsorption parameters given in Table 4, the value of  $n$ , being between 1 and 10, determined from the Freundlich model is indicative of favorable normal adsorption, while the  $K_F$  value gives an idea about the adsorption capacity [28]. Further, the  $1/n$  value,

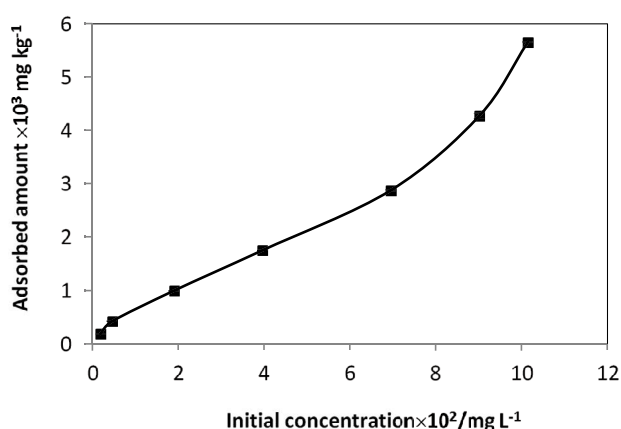


Fig. 6. Amount of phosphate adsorbed on BBC (50.0 mL solutions of different initial concentrations of phosphate shaken with 5.00 g of BBC, 30 min shaking, and 30 min settling time). Error bars are not indicated due to insignificant uncertainty.

being 0.41, implies that about 41% of active adsorption sites have equal energy. The significant surface heterogeneity of BBC would be due to the presence of different types of cations, surface charges and crystal edges on the surface [29]. In the adsorption process, the stronger binding sites are occupied first, until adsorption energy exponentially decreases upon the completion of the adsorption process [30]. Similar characteristics have been reported for adsorption of phosphate on waste material prepared by crushed autoclaved aerated concrete (CAAC) [31], brilliant green on peat [32] and Cd on green coconut shell powder [33]. This model is applied to non-ideal reversible adsorption on heterogeneous surfaces to explain multilayer adsorption, not restricting to the formation of monolayer [34].

The heterogeneity of the BBC surface is further supported by the validity of the D–R isotherm. The saturation capacity ( $q_{max}$ ) determined by this model is 4,531 mg kg<sup>-1</sup>, which is an approximate value for the adsorption capacity, which is significantly higher as compared to previous reports on rice husk and peat, demonstrating the superior ability of BBC for phosphate removal [26,35]. The D–R isotherm assumes no homogeneous surface of the adsorbent, and it is generally applied to express the adsorption mechanism with a Gaussian energy distribution onto a heterogeneous surface [35]. It is noted that the magnitude of  $E$ , mean free energy, is useful for estimating the type of adsorption and if this value is between 8 and 16 kJ mol<sup>-1</sup>, adsorption type can be explained by ion exchange. The mean free energy of 8.00 kJ mol<sup>-1</sup> obtained from the D–R model indicates physical adsorption of phosphate on BBC suggesting that electrostatic forces would play a significant role in adsorption [36], indicating the possibility of removing phosphate species from the solution phase more than what is required to form a monolayer. The excess species either form additional layers or transfer into pores of the brick clay matrix through diffusion [37–40].

Table 1

Standard equations of isotherm models and corresponding regression coefficients ( $R^2$ ) obtained for phosphate removal by BBC [25]

Isotherm model	Standard equations	Equation number	$R^2$
Langmuir	$\frac{1}{q_e} = \frac{1}{q_m} + \frac{1}{q_m K_L} \frac{1}{C_e}$	(2)	0.810
			0.910 (low concentrations – concentrations < 250 mg L <sup>-1</sup> )
Freundlich	$\ln q_e = \frac{1}{n} \ln C_e + \ln K_F$	(3)	0.951
Temkin	$q_e = B \ln K_T + B \ln C_e$	(4)	0.776
	$\ln q_e = \ln q_s - \beta \epsilon^2$	(5)	
Dubnin–Radushkevich	$\epsilon = RT \ln \left[ 1 + \frac{1}{C_e} \right]$	(6)	0.870 (concentrations > 350 mg L <sup>-1</sup> )
	$E = -\frac{1}{\sqrt{2\beta}}$	(7)	

$q_m$  and  $q_e$  are maximum adsorption capacity and equilibrium adsorption capacity;  $C_e$  is the equilibrium concentration of metal ion;  $K_L$ ,  $K_F$ , and  $K_T$  are Langmuir, Freundlich, and Temkin isotherm constants, respectively;  $n$ ,  $B$  are constants, and  $E$  is the mean free energy of adsorption.

Table 2  
Error functions used in isotherm analysis [25,27]

Type of errors	Equations	Equation number
Average relative error (ARE)	$\frac{100}{n} \sum_{i=1}^n \left  \frac{q_{e,\text{meas}} - q_{e,\text{calc}}}{q_{e,\text{meas}}} \right _i$	(8)
Sum square error (SSE)	$\sum_{i=1}^n (q_{e,\text{meas}} - q_{e,\text{calc}})_i^2$	(9)
Hybrid fractional error function (HYBRID)	$\frac{100}{n-p} \sum_{i=1}^n \left  \frac{(q_{e,\text{meas}} - q_{e,\text{calc}})^2}{q_{e,\text{meas}}} \right _i$	(10)
Sum of absolute error (EABS)	$\sum_{i=1}^n  q_{e,\text{meas}} - q_{e,\text{calc}} $	(11)
Non-linear chi-square test ( $\chi^2$ )	$\sum_{i=1}^n \frac{(q_{e,\text{meas}} - q_{e,\text{calc}})^2}{q_{e,\text{meas}}}$	(12)

Table 3  
Values of different error functions associated with isotherm models for phosphate adsorption on brick clay fired at 200°C. High indicates the error values greater than 200

	ARE	SSE	HYBRID	Non-linear chi-square test	EABS
Langmuir	38.243	High	High	High	High
Langmuir (lower concentrations)	41.008	High	High	High	High
Freundlich	18.529	High	High	High	High
D–R (higher concentrations)	26.620	High	High	High	High
Temkin	51.324	High	High	High	High

### 3.4. Kinetics of phosphate adsorption

Kinetics models have been used to investigate the mechanism of adsorption and potential rate-controlling steps, such as chemical reaction, diffusion control and mass transport processes. Kinetics studies, conducted with brick clay fired at 200°C illustrates the variation of the extent of adsorption of phosphate with contact time (Fig. 7). According to Fig. 7, the rate of adsorption is more at the initial stage, which gradually decreases and remains almost constant after the optimum time period.

Linearized integrated forms of different kinetics models, namely pseudo-first-order, pseudo-second-order and Elovich, were applied to investigate the rate of adsorption of phosphate species. Different diffusion models, namely the external mass transfer diffusion model, McKay and Poots intraparticle diffusion models, Weber and Morris intraparticle diffusion model, and Boyd model, were applied in order to identify whether the adsorption mechanism is particle diffusion or film diffusion. Diffusion models provide a better understanding of the process of transferring phosphate from the liquid phase to solid phase and determining rate-limiting step [42]. Table 5 gives equations related to the models mentioned above, where  $k'$  is the apparent rate constant,  $t$  is contact time,  $q_e$  and  $q_i$  are the

Table 4  
Isotherm constants obtained for the removal of phosphate from BBC (50.0 mL phosphate, 5.00 g of BBC)

Isotherm model	Parameter	Values
Freundlich	$K_f$ (mg g <sup>-1</sup> )	221
	$n$	2.39
	$q_{\text{max}}$ (mg kg <sup>-1</sup> )	4,531
D–R (concentration > 100 mg L <sup>-1</sup> )	$\beta$ (mol <sup>2</sup> kJ <sup>-2</sup> )	0.0078
	$E$ (kJ mol <sup>-1</sup> )	8.00

masses of phosphate species sorbed by unit mass of sorbent at equilibrium and at time  $t$ ,  $C_t$  and  $C_0$  are phosphate ion concentrations in solution at time  $t$  and at  $t = 0$ ,  $\alpha$  is the initial adsorption rate and  $\beta$  is related to the extent of surface coverage,  $\beta_L$  is the liquid–solid mass transfer coefficient,  $S$  is the specific surface area for mass transfer,  $X_i$  is the thickness of the boundary layer,  $k'$  is the rate constant,  $R$  is the percentage adsorption of phosphate,  $n$  is the gradient of linear plots, and  $k_{\text{id}}$  is the intra-particle diffusion rate constant.

Results of adsorption kinetics data for linearized pseudo-first-order, pseudo-second-order and Elovich model (Fig. 8), clearly show the validity of the pseudo-second-order model,

supporting the regression coefficient ( $R^2$ ) value being close to 1. Accordingly, the pseudo-second-order rate constant ( $k'$ ) and initial adsorption rate ( $h_0$ ) are determined to be  $2.25 \times 10^{-2} \text{ kg mg}^{-1} \text{ min}^{-1}$  and  $156 \text{ mg kg}^{-1} \text{ min}^{-1}$ .

The validity of pseudo-second-order kinetics model for adsorption of phosphate on BBC indicates that there should be two types of reactive moieties for phosphate-BBC interaction. The order of variation of the adsorption rate determined based on kinetics, which depends on the path to reach equilibrium, is not in agreement with the extent of removal of phosphate ions determined when the system has reached equilibrium, due to the fact that kinetics and equilibrium aspects are not inter-dependent. The pseudo-second-order model describes that the rate-determining step of sorption suggests chemisorption

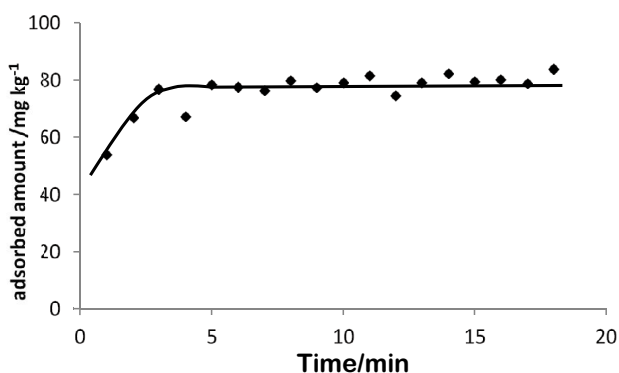


Fig. 7. Variation of the amount of phosphate adsorbed with contact time (50.0 mL of  $10 \text{ mg L}^{-1}$  phosphate solution, 5.0 g of BBC, 20 separate samples used for the analysis).

Table 5  
Standard equations of kinetics and diffusion models [36,43]

Kinetic model	Standard equations	Equation number	$R^2$
Pseudo-first-order	$\log(q_e - q) = \log q_e - \left(\frac{k_1}{2.303}\right)t$	(13)	0.429
Pseudo-second-order	$\frac{t}{q_t} = \frac{1}{q_e}t + \frac{1}{(k'q_e^2)}$	(14)	0.996
Initial adsorption rate ( $h_0$ )	$h_0 = k'q_e^2$	(15)	
Elovich model	$q_t = \frac{1}{\beta} \ln(\alpha\beta) + \frac{1}{\beta} \ln t$	(16)	0.747
External mass transfer diffusion model	$\frac{C_t}{C_0} = -\beta_L St$	(17)	0.498
McKay and Poots intra-particle diffusion model	$q_t = X_i + k't^{0.5}$	(18)	0.613
Webber and Morris intra-particle diffusion model	$\log R = \log k_{id} + n \log(t)$	(19)	0.725
Boyd model	$B_t = -0.4977 - \ln\left(1 - \left[\frac{q_t}{q_e}\right]\right)$ vs. $t$	(20)	0.504

involving sharing or exchange of electrons between the adsorbate and the adsorbent.

Diffusion models describe the process of transferring of adsorbate from the liquid phase to the solid phase and determining the rate-limiting step [44]. Analysis of phosphate adsorption results indicates that none of the diffusion models given in Table 5 is in agreement with adsorption of phosphate on BBC, suggesting that contribution from diffusion is not significant for mass transfer.

### 3.5. Desorption of phosphate from the adsorbent

Desorption experiments carried out by varying initial solution pH indicate that desorption increases with an increase in pH BBC suspension; but it is very low for the whole range of pH investigated (Fig. 9). Therefore, desorption experiments confirm that phosphate ions adsorbed would not leach to the environment under normal conditions.

### 3.6. Adsorption mechanism

It is thus believed that the mass transfer of phosphate species on and within the BBC phase is probably due to the combination of many modes of mass transfer from the solution phase to the solid adsorbent phase. The process may follow physisorption which partially affects the precipitation due to different cations leached. Further, parameters obtained for different adsorbents based on the Freundlich adsorption isotherm demonstrate the superior nature of brick clay on the removal of phosphate (Table 6). Although it is difficult to decide on a single rate-determining step, according to the experimental findings and adsorbent structure and surface properties, the adsorption mechanism of phosphate onto BBC may be assumed to involve the following steps:

Table 6  
Adsorption performance of different adsorbents in removal of phosphate-based on the Freundlich adsorption isotherm

Adsorbent	$R^2$	$K_F$	$1/n$	$n$	Shaking time/min	Settling time/min	Ref
Crushed autoclaved aerated concrete – CAAC	0.995	22.2	0.94	1.06	240	20	[31]
Aleppo pine adsorbent	0.968	0.889	0.78	1.28	40	–	[41]
Calcined waste egg shell	0.964	23.02	1.26	0.76	60	–	[38]
Skin split waste (SSW) – Al	0.950	18.66	0.31	3.20	120	–	[3]
Skin split waste (SSW) – Fe	0.950	2.46	0.37	2.70	120	–	[3]
Brick clay	0.951	221	0.41	2.43	30	30	This study

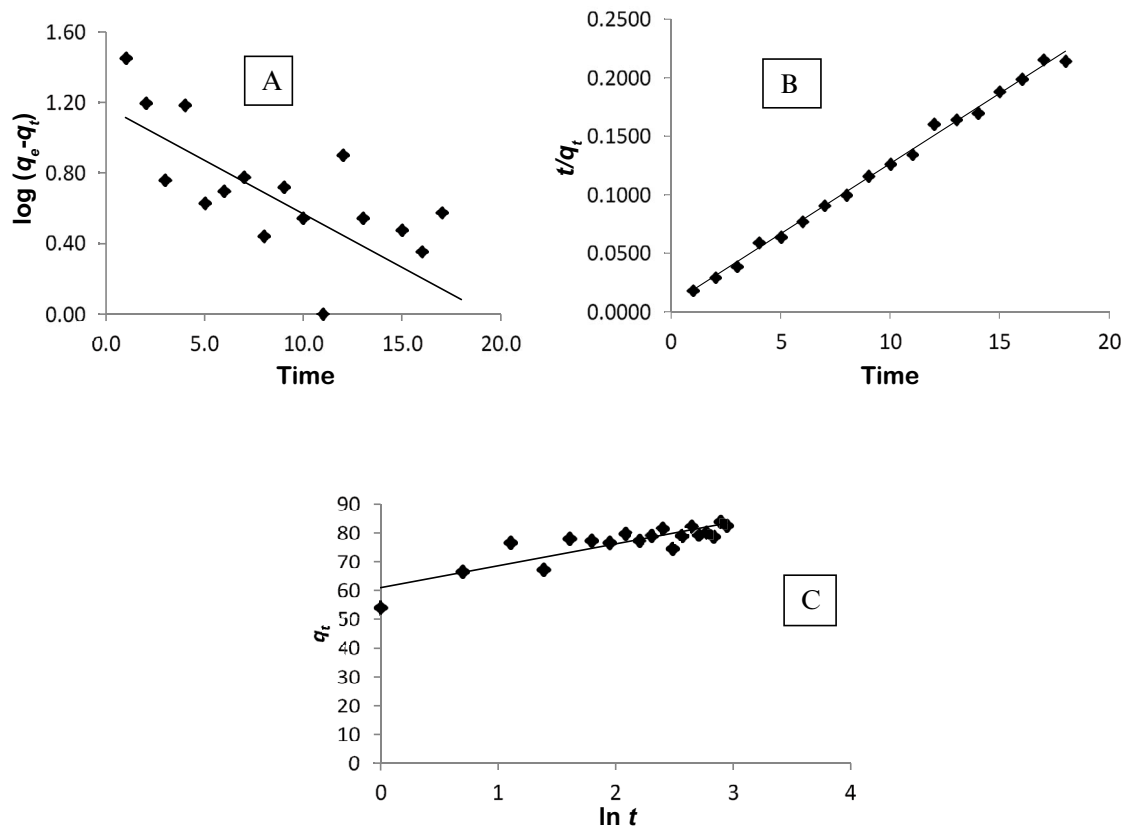


Fig. 8. Adsorption kinetics studies for removal of phosphate from brick clay: (a) pseudo-first-order kinetics, (b) pseudo-second-order kinetics, (c) Elovich model (50.0 mL of 10 mg L<sup>-1</sup> phosphate solution, 5.00 g of BBC)  $t$  is given in min and  $q_t$  is given in mg kg<sup>-1</sup>.

- Mass transfer from the bulk solution on to boundary film, and then on to the surface of the adsorbent via particle diffusion.
- Mass transfer due to species concentration gradient in the mixture and random molecular motion. This results in uniform concentration in both phases. This step may occur in any adsorption system.
- Acceleration of the whole mass transfer process may be due to the release of cations to the solution phase which supplies vacant sites for the reaction. Further, cationic particles may result in strong bonds with PO<sub>4</sub><sup>3-</sup>.
- Large surface area (reported in the literature for the same adsorbent) would benefit to enhance adsorption capacity.

#### 4. Conclusion

Brick clay particles burnt at 200°C (BBC) shows high phosphate removal (87%) from 10.0 mg L<sup>-1</sup> phosphate solution at 1:10 adsorbent/solution ratio under the optimized conditions. The Freundlich model indicates that 45% of active adsorption sites have equal energy levels; the surface heterogeneity of BBC is due to the presence of different types of cations, surface charges, and crystal edges on brick clay all of which are favorable toward sorption. The D–R isotherm model describes the adsorption of phosphate on the heterogeneous BBC surface which fits better at higher concentrations. The mean free adsorption energy ( $E$ ) of 1.12 kJ mol<sup>-1</sup> indicates physical adsorption of phosphate

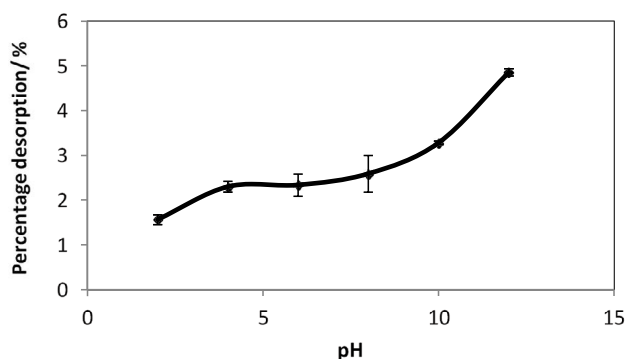


Fig. 9. Extent of desorption of phosphate pre-adsorbed on BBC for different initial solution pH.

on BBC at high concentrations. Pseudo-second-order kinetics results in an apparent rate constant of  $22.5 \text{ g mg}^{-1} \text{ min}^{-1}$ . Diffusion models are not satisfactorily obeyed indicating that intraparticle diffusion is not the sole rate-limiting step, and further, surface adsorption and intraparticle diffusion would simultaneously occur during interaction of phosphate with BBC particles.

#### Acknowledgments

Financial support through a research grant by the National Science Foundation (RG/2012/BS/05) is greatly appreciated.

#### Symbols

$C_i$	—	Initial concentration
$C_f$	—	Final concentration
BBC	—	Brick clay particles burnt at $200^\circ\text{C}$
$q_m$	—	Maximum adsorption capacity
$q_e$	—	Equilibrium adsorption capacity
$C_e$	—	Equilibrium concentration of metal ion
$K_L$	—	Langmuir isotherm constant
$K_F$	—	Freundlich isotherm constant
$K_T$	—	Temkin isotherm constant
$n, B$	—	Constants
$E$	—	Mean free energy of adsorption
$k'$	—	Apparent rate constant
$t$	—	Contact time
$q_e$	—	Mass of phosphate species sorbed by unit mass of sorbent at equilibrium
$q_t$	—	Mass of phosphate species sorbed by unit mass of sorbent at time $t$
$C_t$	—	Phosphate ion concentrations in solution at time $t$
$C_0$	—	Phosphate ion concentrations in solution at time $t = 0$
$\beta_L$	—	Liquid–solid mass transfer coefficient
$S$	—	Specific surface area for mass transfer
$X_i$	—	Thickness of the boundary layer
$k'$	—	Rate constant
$R$	—	Percentage adsorption of phosphate
$n$	—	Gradient of linear plots
$k_{id}$	—	Intra-particle diffusion rate constant
$h_0$	—	Initial adsorption rate

#### References

- [1] A.M. Zayed, N. Terry, Chromium in the environment: factors affecting biological remediation, *Plant Soil*, 249 (2003) 139–156.
- [2] M. Rathod, K. Mody, S. Basha, Efficient removal of phosphate from aqueous solutions by red seaweed, *Kappaphycus alvarezii*, *J. Cleaner Prod.*, 84 (2014) 484–493.
- [3] X. Huang, X. Liao, B. Shi, Adsorption removal of phosphate in industrial wastewater by using metal-loaded skin split waste, *J. Hazard. Mater.*, 166 (2009) 1261–1265.
- [4] S. Jellali, M.A. Wahab, M. Anane, K. Riahi, L. Bousselmi, Phosphate mine wastes reuse for phosphorus removal from aqueous solutions under dynamic conditions, *J. Hazard. Mater.*, 184 (2010) 226–233.
- [5] E. Nassef, Removal of phosphates from industrial wastewater by chemical precipitation, *Eng. Sci. Technol. Int. J.*, 2 (2012) 409–413.
- [6] C.W. Purnomo, A. Prasetya, The study of adsorption breakthrough curves of Cr(VI) on bagasse fly ash (BFA), *Proc. World Congr. Eng. Comput. Sci.*, 2 (2007) 24–26.
- [7] D. Sud, G. Mahajan, M.P. Kaur, Agricultural waste material as potential adsorbent for sequestering heavy metal ions from aqueous solutions – a review, *Bioresour. Technol.*, 99 (2008) 6017–6027.
- [8] T.K. Naiya, P. Chowdhury, A.K. Bhattacharya, S.K. Das, Saw dust and neem bark as low-cost natural biosorbent for adsorptive removal of Zn(II) and Cd(II) ions from aqueous solutions, *Chem. Eng. J.*, 148 (2009) 68–79.
- [9] L. Hang, S. Hong, J. He, F. Gan, Y.S. Ho, Adsorption characteristic studies of phosphorus onto laterite, *Desal. Water Treat.*, 25 (2011) 98–105.
- [10] V.T.L. Bogahawatta, A.B. Poole, The influence of phosphate on the properties of clay, *Appl. Clay Sci.*, 10 (1996) 461–475.
- [11] L. Madrid, A.M. Posner, Desorption of phosphate from goethite, *Soil Sci.*, 30 (1979) 697–707.
- [12] Y.S.R. Chen, J. Butler, W. Stumm, Kinetic study of phosphate reaction with aluminum oxide and kaolinite, *Environ. Sci.*, 7 (1973) 327–332.
- [13] D. Gu, X. Zhu, T. Vongsay, M. Huang, Phosphorus and nitrogen removal using novel porous bricks incorporated with wastes and minerals, *Pol. J. Environ. Stud.*, 22 (2013) 1349–1356.
- [14] N. Priyantha, A. Bandaranayaka, Optimization of parameters for effective removal of Cr(VI) species by burnt brick clay, *J. Natl. Sci. Found. Sri Lanka*, 38 (2010) 109–114.
- [15] N. Priyantha, A. Bandaranayaka, Interaction of Cr(VI) species with thermally treated brick clay, *Environ. Sci. Pollut. Res.*, 18 (2011) 75–81.
- [16] K.Y. Foo, B.H. Hameed, Insights into the modeling of adsorption isotherm systems, *Chem. Eng. J.*, 156 (2010) 2–10.
- [17] C. Senevirathna, N. Priyantha, Correlation between firing temperature and defluoridation capacity of brick clay, *Int. J. Glob. Environ. Issues*, 9 (2009) 239–248.
- [18] N. Priyantha, S. Perera, Removal of sulfate, phosphate and colored substances in wastewater effluents using feldspar, *Water Resour. Manage.*, 14 (2000) 417–433.
- [19] E. Pehlivan, A.M. Ozkan, S. Dinc, S. Parlayisi, Adsorption of  $\text{Cu}^{2+}$  and  $\text{Pb}^{2+}$  ion on dolomite powder, *J. Hazard. Mater.*, 167 (2009) 1044–1049.
- [20] N. Priyantha, S. Keerthirathna, I. Lokuge, H. Gajanayake, Removal of blue colouration from industrial effluents by burnt-brick particles, *J. Natl. Sci. Found. Sri Lanka*, 28 (2001) 287–299.
- [21] D.A. Tessema, D.D. Alemayehu, A comparative study on  $\text{Pb}^{2+}$  removal efficiencies of fired clay soils of different particle size distributions, *Afr. J. Environ. Sci. Technol.*, 7 (2013) 824–832.
- [22] V. Njoku, E.E. Oguzie, C. Obi, O.S. Bello, A. Ayuk, Adsorption of copper(II) and lead(II) from aqueous solutions onto a Nigerian natural clay, *Aust. J. Basic Appl. Sci.*, 5 (2011) 346–353.
- [23] M. Thommes, K. Kaneko, A.V. Neimark, J.P. Olivier, F. Rodriguez-Reinoso, J. Rouquerol, K.S.W. Sing, Physisorption of gases, with special reference to the evaluation of surface

- area and pore size distribution (IUPAC Technical Report), Pure Appl. Chem., 87 (2015) 1051–1069.
- [24] K. Vijayaraghavan, T.V.N. Padmesh, K. Palanivelu, M. Velan, Biosorption of nickel(II) ions onto *Sargassum wightii*: application of two-parameter and three-parameter isotherm models, J. Hazard. Mater., 133 (2006) 304–308.
- [25] L.B.L. Lim, N. Priyantha, N.H.M. Mansor, Utilizing *Artocarpus altilis* (breadfruit) skin for the removal of malachite green: isotherm, kinetics, regeneration, and column studies, Desal. Water Treat., 57 (2015) 16601–16610.
- [26] H.I. Chieng, L.B.L. Lim, N. Priyantha, Enhancing adsorption capacity of toxic malachite green dye through chemically modified breadnut peel: equilibrium, thermodynamics, kinetics and regeneration studies, Environ. Technol., 36 (2015) 86–97.
- [27] I.D. Mall, V.C. Srivastava, N.K. Agarwal, Removal of Orange-G and Methyl Violet dyes by adsorption onto bagasse fly ash - kinetic study and equilibrium isotherm analyses, Dyes Pigm., 69 (2006) 210–223.
- [28] G.O. El-sayed, Removal of methylene blue and crystal violet from aqueous solutions by palm kernel fiber, Desalination, 272 (2011) 225–232.
- [29] U.R. Lakshmi, V.C. Srivastava, I.D. Mall, D.H. Lataye, Rice husk ash as an effective adsorbent: evaluation of adsorptive characteristics for Indigo Carmine dye, J. Environ. Manage., 90 (2009) 710–720.
- [30] J. Zeldowitsch, Adsorption site energy distribution, Acta Phys. Chim. URSS, 1 (1934) 961–973.
- [31] S. Malavipathirana, S. Wimalasiri, N. Priyantha, S. Wickramasooriya, A. Welagedara, G. Renman, Value addition to waste material supported by removal of available phosphate from simulated brackish water—a low cost approach, J. Geosci. Environ. Prot., 1 (2013) 7–12.
- [32] H.I. Chieng, N. Priyantha, L.L.B. Lim, Effective adsorption of toxic brilliant green from aqueous solution using peat of Brunei Darussalam: isotherm, kinetics and regeneration studied, RSC Adv., 5 (2015) 34603–34615.
- [33] G.H. Pino, L.M.S. de Mesquita, M.L. Torem, G.A.S. Pinto, Biosorption of cadmium by green coconut shell powder, Miner. Eng., 19 (2006) 380–387.
- [34] S. Wang, Z.H. Zhu, Characterisation and environmental application of an Australian natural zeolite for basic dye removal from aqueous solution, J. Hazard. Mater., 136 (2006) 946–952.
- [35] A.O. Dada, A.P. Olalekan, A.M. Olatunya, O. Dada, Langmuir, Freundlich, Temkin and Dubinin–Radushkevich isotherms studies of equilibrium sorption of  $Zn^{2+}$  onto phosphoric acid modified rice husk, IOSR J. Appl. Chem., 3 (2012) 38–45.
- [36] V. Vadivelan, K. Vasanth Kumar, Equilibrium, kinetics, mechanism, and process design for the sorption of methylene blue onto rice husk, J. Colloid Interface Sci., 286 (2005) 90–100.
- [37] S. Chatterjee, D.S. Lee, M.W. Lee, S.H. Woo, Nitrate removal from aqueous solutions by cross-linked chitosan beads conditioned with sodium bisulfate, J. Hazard. Mater., 166 (2009) 508–513.
- [38] T.E. Köse, B. Kivanc, Adsorption of phosphate from aqueous solutions using calcined waste eggshell, Chem. Eng. J., 178 (2011) 34–39.
- [39] T.S. Singh, K.K. Pant, Equilibrium, kinetics and thermodynamic studies for adsorption of As(III) on activated alumina, Sep. Purif. Technol., 36 (2004) 139–147.
- [40] M. Mahramanlioglu, I. Kizilcikli, I.O. Bicer, Adsorption of fluoride from aqueous solution by acid treated spent adsorption of fluoride from aqueous solution by acid treated spent adsorption of fluoride from aqueous solution by acid treated spent bleaching earth, J. Fluorine Chem., 1139 (2002) 3–9.
- [41] S. Benyoucef, M. Amrani, Adsorption of phosphate ions onto low cost Aleppo pine adsorbent, Desalination, 275 (2011) 231–236.
- [42] L.B.L. Lim, N. Priyantha, M.H.F. Lai, R.M. Salleha, T. Zehra, Utilization of *Artocarpus* hybrid (Nanchem) skin for the removal of Pb(II): equilibrium, thermodynamics, kinetics and regeneration studies, Int. Food Res. J., 22 (2015) 1043–1052.
- [43] S.A. Odoemelam, C.U. Iroh, J.C. Igwe, Copper(II), cadmium(II) and lead(II) adsorption kinetics from aqueous metal solutions using chemically modified and unmodified cocoa pod husk (*Theoproma cacao*) waste biomass, Res. J. Appl. Sci., 6 (2011) 44–52.
- [44] G. Mckay, V.J.P. Poots, Kinetics and diffusion processes in colour removal from effluent using wood as an adsorbent, J. Chem. Technol. Biotechnol., 30 (1980) 279–292.